Journal of Magnetism and Magnetic Materials 572 (2023) 170603

Contents lists available at ScienceDirect

Journal of Magnetism and Magnetic Materials

journal homepage: www.elsevier.com/locate/jmmm

Magnetorheological brushes – Scarcely explored class of magnetic material

A.K. Bastola [a,b,*], M Gannavarapu [a], L.A. Parry [b], M. Shrestha [c]

[a] School of Mechanical and Aerospace Engineering, Nanyang Technological University, 50 Nanyang Avenue, Singapore 639798, Singapore
[b] Centre for Additive Manufacturing (CfAM), Faculty of Engineering, University of Nottingham, Nottingham NG8 1BB, United Kingdom
[c] Continental-NTU Corporate Laboratory, Nanyang Technological University, Singapore 117411, Singapore

ARTICLE INFO

Keywords:
Magnetorheological brush
Magnetorheological fluid
Magnetorheological elastomer
Magnetic field
Magnetoactive materials

ABSTRACT

Magnetic materials such as magnetorheological (MR) fluids, and magnetorheological elastomers exhibit a broad change in their material properties, for example, viscosity and storage modulus in the presence of a magnetic field. Studies related to such MR fluid and elastomer materials are extensively available. The MR brush, meanwhile, is less frequently explored and understood. An MR brush is defined by the brush-like structures formed from chains of magnetic particles embedded within a carrier matrix, typically fluids or elastomers. In this study, we explore magnetorheological fluid (MRF) brush and magnetorheological elastomer (MRE) brush and investigate their magneto-mechanical properties. The investigation measured the stiffness and the MR response, defined as the change in properties in the presence of a magnetic field for MRF and MRE brushes. Further dependence of the magnetic effect on material and preparation parameters, mainly concentration of magnetic particles and curing flux density (for MRE brush) were investigated. The responsiveness of the brushes is compared using the Magnetorheological response index, as a proposed metric in this study. The results indicate that the MRE brush possess a greater absolute stiffness, but a lower MR response than that of the MRF brush. Both MRF and MRE brushes show an increase in the MR response with an increased concentration of magnetic fillers. MRE brush further demonstrate an enhanced MR response, which could be highly comparable to MRF brush coinciding with an increase in the magnetic flux density during the curing process. The fundamental investigation of both solid and fluid MR brushes in this study opens a new avenue in the area of magnetic materials. This new class of magnetically controllable materials could potentially be employed in applications where soft and tuneable bristle-like structures are desired.

1. Introduction

Magnetic composite materials are structurally composed of magnetic micro/nano-sized particles dispersed in a carrier medium [1-9]. They are broadly classified into fluids and solids (e.g., elastomers) based on the physical state of the carrier medium in the absence of a magnetic field [3,5,10-17].

In recent years, magnetic materials have attracted wide attention amongst diverse fields resulting in tremendous progress in terms of materials development, in particular amongst composites. Exploration of various matrices and magnetic fillers [11,18-20], as well as fabrication routes including traditional moulding, digital processes and 3D printing [11,21-24], to enhance the performance of the magnetoactive composites can be witnessed. Their potential has wide-reaching applications amongst, but not limited to robotics, biomedical and civil engineering [1,11,25-27] due to the advantages such as remote contactless actuation, high actuation strain and strain rate, self-sensing, and instantaneous response offered by these multifunctional materials. Nevertheless, despite increased adoption, a comprehensive understanding of the magneto-mechanical response remains necessary for taking full advantage of various functionalities offered by these materials.

MR fluids (MRF) are materials with a fluid carrier medium such as mineral oil and hydrocarbon oil [28]. MR elastomers (MRE) are particle-reinforced composites consisting of a carrier medium using a solid elastomer such as silicone elastomer, natural rubber and other polymers [1,10,12]. MRF are versatile because they can reversibly change their physical state from a liquid to a semi-solid under an external magnetic field. This change is accomplished through the change in viscosity by several orders of magnitude due to magneto-induced interaction and alignment of the magnetic particles. Due to such significant and reversible transitions, MRF have broad industrial applications in

* Corresponding author at: Centre for Additive Manufacturing (CfAM), Faculty of Engineering, University of Nottingham, Nottingham NG8 1BB, United Kingdom.
E-mail address: anil.bastola@nottingham.ac.uk (A.K. Bastola).

https://doi.org/10.1016/j.jmmm.2023.170603
Received 18 January 2023; Received in revised form 24 February 2023; Accepted 5 March 2023
Available online 9 March 2023
0304-8853/© 2023 The Author(s). Published by Elsevier B.V. This is an open access article under the CC BY-NC-ND license (http://creativecommons.org/licenses/by-nc-nd/4.0/).

engineering and are found in shock absorbers, clutches, seismic protection devices, and braking systems for high-performance automobiles [28-30].

A major issue of MRF, however, is the gradual sedimentation of the magnetic particles suspended in the carrier medium. In MRF, the magnetic particles are free to move around in the carrier fluid in the absence of a magnetic field. In this state, the greater influence of gravitational force causes the particles to segregate. Other problems include corrosion of the magnetic particles due to oxidation and thickening of the MRF over time. These problems cause material instability and the responsiveness of the MRF deteriorates. Thus, MRFs are not highly durable and require periodic replacement.

MR elastomers (MRE) have the ability to reversibly change their properties such as elastic moduli and shape at micro-/milli- scales and are the solid analogue to MRF. MRE are composed of elastomers with magnetic particles embedded within the elastomer matrix. Thus, MRE function as elastomers with magnetic field responsiveness [2,11,14,31,32]. The properties of the MRE are further dependent on the distribution and orientation of the magnetic particles that are either random or ordered within the matrix [10,33,34]. Applications of MRE include vibration absorbers, force sensors and actuators [2]. If a magnetic field is applied during the curing process, particles preferentially align to the magnetic flux direction and the resulting material becomes anisotropic. Curing in the absence of a magnetic field tends to produce isotropic material properties [10,14]. MRE do not exhibit the problems associated with MRF, such as sedimentation and corrosion, because the magnetic particles are restrained by cross-links of the polymer matrix.

Upon application of a magnetic field onto an MRF, the magnetic particles align and form chain-like structures in the direction of the applied magnetic field. This structure resembles a brush with the particle chains functioning as the bristles [35-38]. This type of brush is known as a magnetorheological (MR) brush. The key distinguishing feature of the MR brush is its free-standing bristles which are not confined within an enclosed volume typical of MRF nor a fully solid structure like MRE. The fine structures of magnetorheological brushes have been exploited in magneto-abrasive finishing, which are able to achieve nanometre surface finishes with nominal surface damage [35,36,39-42] and as well in soft robotics [43,44]. Despite their advantages, MRFs alone, are susceptible to instability and the inhabitation of corrosion remains challenging. Therefore, it is worthy of investigation to explore the development of MRE brushes as a promising alternative to MRF brushes owing to their better stability and durability offered by MRE [37,45]. However, very limited studies are reported on MR brushes and this area remains greatly unexplored. Although MRE brushes could offer better stability compared to MRF brushes, a comparison between solid and fluid MR brushes has never been previously attempted. Furthermore, the mechanism of bristle formation and the performance of MR brushes such as thickness, shape, and height of the bristles with respect to the filler loading and applied magnetic flux density have not been reported yet. Such fundamental investigation is necessary to unleash the potential that the MR brush could offer. MR brushes are mostly characterized by their effective stiffness and the MR response, which is a measure of the change in effective stiffness due to the applied magnetic field.

Soft robotics is an increasingly developing field with numerous potential applications, including biomedical devices and human-robot interactions. Magnetic field responsive materials are a particularly promising class of materials for creating flexible humanoid robots due to their two way actuation, quick responsiveness and flexibility of the matrix material [46,47]. These magnetic field responsive materials are programmable with the ability to respond to external magnetic fields, enabling new functionalities such as tuneable stiffness or shape-morphing capabilities. Moreover, Additive Manufacturing (AM), also referred as 3D printing, is a layer-by-layer manufacturing process that enables designers to incorporate geometrical complexity and multi-materials into their parts to embed multifunctionality not achievable by conventional manufacturing means [48-51]. AM can be utilized to fabricate the complex structures of MR brushes without requiring the application of a magnetic field, as in conventional forming techniques. A recently reported computationally guided direct ink writing AM technique has the potential to fabricate highly controlled MR structures by slowly converting MR fluid to MR elastomer during the process in a controlled fashion [52].

This study pursues to contribute to the research on MR brushes, a class of magnetic materials largely unexplored in the literature. It focuses to understand their magneto-mechanical properties and their dependence on material and preparation parameters. In the experimental study, samples of MRF and MRE brushes were prepared, and their MR performance was investigated and compared. The magneto-rheological response of MR brushes using compression testing with samples subjected to an external magnetic field has been explored. The MR response was studied in relation to the concentration of magnetic particle loading, compression rate and magnetic flux density.

2. Materials and methodology

Silicone oil (AP1000, Sigma-Aldrich, Singapore), elastomer (SS-6B, Silicone Solutions, USA) and carbonyl iron particles (44890, Sigma-Aldrich, Singapore) were used as received. The silicone oil has a viscosity of 800–1200 mPas at 25 °C and the elastomer has a durometer of 30 Shore A, a tensile strength of 1.37 MPa, and an elongation at break of 250% after curing, according to the supplier.

The MRF brush samples were prepared with concentrations starting from 50 wt.% in increments of 10 to 80 wt.% of carbonyl iron powders (CIP) (5–9 μm sized spherical particles as per supplier). Silicone oil and CIP were thoroughly mixed mechanically and subsequently agitated by sonication in a water bath for 30 min, with the aim to provide a homogenous suspension. See Fig. 1.

The MRE brush samples were prepared at the same concentrations as the MRF brush with an additional step of the curing process. The composite resin was cast into a mould, where a magnetic field can be applied to form columnar chains of magnetic particles to produce the bristle-like structure. The sample remained undisturbed at 25 °C for 24 h for the elastomer to cure completely, as per the supplier's specification. Moreover, this casting process was repeated at three different magnetic flux densities across the four different concentrations of CIP used.

A simple experimental apparatus was conceived and manufactured, as shown in Fig. 2. The apparatus provides a controlled and adjustable range of magnetic flux densities during the curing phase casting MRE samples, and the compression tests performed on both the MRF and MRE samples. A solid cubic NdFeB permanent magnet (25 mm × 25 mm × 25 mm) was used to generate the magnetic field. For the apparatus, the chosen magnetic flux density was maintained by the adjustment of the gap between the permanent magnet and the spacer. The magnetic flux values reported were measured at three different locations on the top surface of the magnetic field generator exactly above the permanent magnet (three equally spaced points: centre, midway and edge) and the average value obtained are given in Table 1.

In the investigation, three magnetic flux density values were used and referred as Low, Med, and High for convenience. The same convention will be followed in graphs and tables. A Gaussmeter (MG-801, Magna, Japan), with a reported resolution of 0.1 mT was used to measure the magnetic flux of the magnetic generator. MRF or MRE brushes were placed onto the magnetic field generator and transferred to a universal testing machine (Instron 5569) for compression testing. The Instron machine was equipped with a 500 N load cell and the upper fixture of the universal testing machine was replaced by a non-magnetic aluminium fixture to compress the samples.

For the MRF brush, confined testing was conducted, whereby MR fluid was enclosed within an annular ring (Fig. 2). The inner radius of the ring was 17 mm with a thickness of 1 mm, which yielded an enclosed volume of approximately 1 ml. For the MRF brush, 1 ml of the fluid was

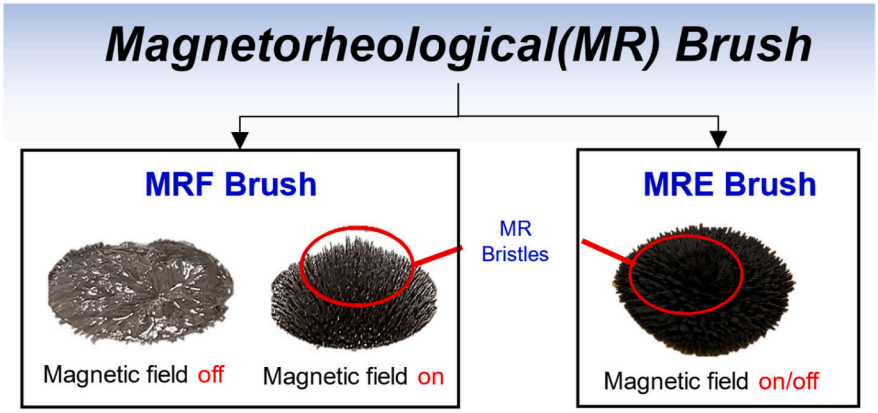

Fig. 1. Scheme of the work: MRF columnar bristles form only in the presence of a magnetic field, while MRE columnar bristles persist in both the absence and presence of a magnetic field.

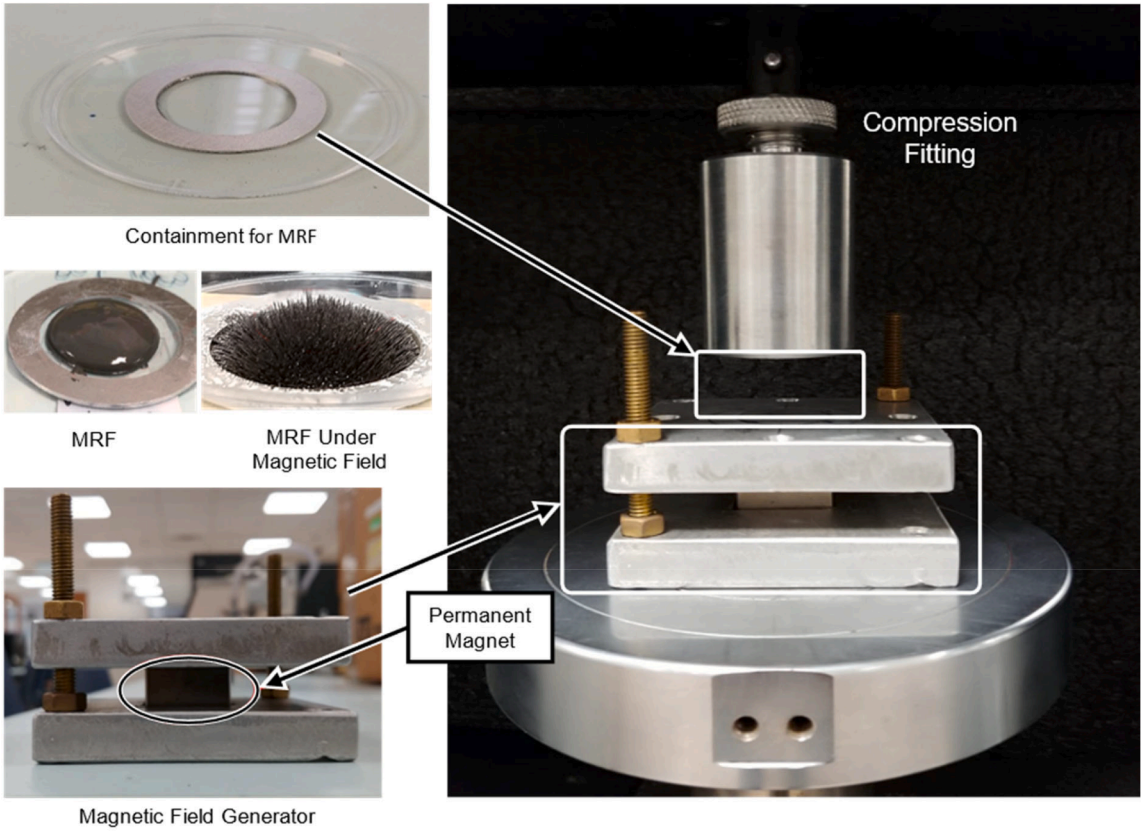

Fig. 2. Experimental apparatus.

Table 1
The measured average magnetic flux densities generated by the magnetic field generator apparatus used during the curing of the MRE brushes and compression testing of both MRF and MRE samples.

Magnetic test configuration (Notation)	Average magnetic flux density (T)
Low Field	0.199
Med Field	0.313
High Field	0.511

measured using a syringe and dispensed onto a Petri dish. The non-magnetic aluminium ring adhered to the Petri dish prevented the fluid from spilling over. Also note the MRE brush samples were created with the same volume (i.e., 1 ml mixture of CIP and elastomer resin) as that of the MRF brush to provide a direct experimental comparison.

Samples were compressed until the upper compression plate reached 1.1 mm height from the bottom plate and applied for both MRF and MRE brushes. The magnetorheological material is viscoelastic in nature [14], therefore, the response of the MR brushes was expected to be strain rate dependent. Thus, the testing was performed at four different compression rates (12, 30, 60, 90) mm/min on the MRF samples.

In total, four different concentrations of CIP (50, 60, 70, 80) wt.% were prepared for both MRF and MRE brushes, with the MRE cured at three different magnetic fields (Low, Med, and High). In total, three samples for each MRF and MRE brush configuration were considered, and the expressed results are the average of three samples.

3. Results and discussion

3.1. Magnetorheological fluid brushes

The response of MRF brushes amongst selected configurations subjected to varying magnetic fields and compression rates are shown in Fig. 3. It is observed that the force-displacement response is predominantly influenced by the strength of the magnetic field and the concentration of CIP. The effect of strain rate on samples, as shown across 50 wt.% and 80 wt.% in Fig. 3a, indicates the MRF brushes are apparently insensitive to the applied strain rate.

Compression testing reveals insight into the formation of bristle structures across different magnetic flux densities. The bristle height is indicated by the maximum displacement during compression, as shown in Fig. 3, when the upper compression plate reached the lower point (i.e., 1.1 mm above the bottom platform). Variation in the MR bristle height was more pronounced for the higher concentration of CIP. The longer but weaker bristles were formed at low magnetic flux, while relatively shorter but stiffer bristles were formed at a higher magnetic flux density (Fig. 3b-i & b-ii).

The magnetorheological (MR) response is defined as the change in properties of MR materials in the presence of a magnetic field. A method for evaluating the MR response of MRF brushes is determined by comparing their stiffness. The tangent modulus is typically used to characterize the viscoelastic materials or those with non-linear stress/strain response such as MR materials [10,53]. The tangent modulus represents the material's instantaneous stiffness and is derived from slope of the stress-strain curve at the given strain. The geometry of the brush structures is not easily defined, so the analysis focuses on stiffness rather than modulus. To determine stiffness, a method similar to obtaining tangent modulus across the entire force-displacement response is used, and the maximum stiffness value is selected for analysis.

The graphs presented in Fig. 3 show the relationship between force and displacement of MR brushes subjected to compression. Fig. 3ai and 3aii demonstrate the impact of compression rate on samples with 50 wt.% and 80 wt.% CIP concentration, respectively, at High field. Fig. 3bi and 3bii shows the effect of filler concentration on samples in the presence of Low and High field. Observations about the peak force and maximum displacement (i.e., bristle height) may be seen. It is apparent that the strain rate does not have a noticeable effect on the response for a fixed CIP concentration. However, as seen in Fig. 3bi, the trend of the curve is distinct and influenced greatly by the CIP concentrations used. Higher concentration of CIPs leads to higher peak load and the formation of longer bristles. The reported absolute stiffness across the MRF brushes and magnetic fields are shown in Fig. 4. The stiffness was not significantly dependent on the compression rates for all the samples. Hence, the compression rate of 60 mm/min was chosen for the subsequent comparisons and discussions for the remainder of this investigation. Rather, the effect of magnetic field and concentration of CIP have a more profound effect.

Therefore, the concentration of the magnetic particles is of high significance for the MR response in MRF brushes. As shown in Fig. 3 (b-i & b-ii) and Fig. 4, the CIP concentration has a considerable impact on

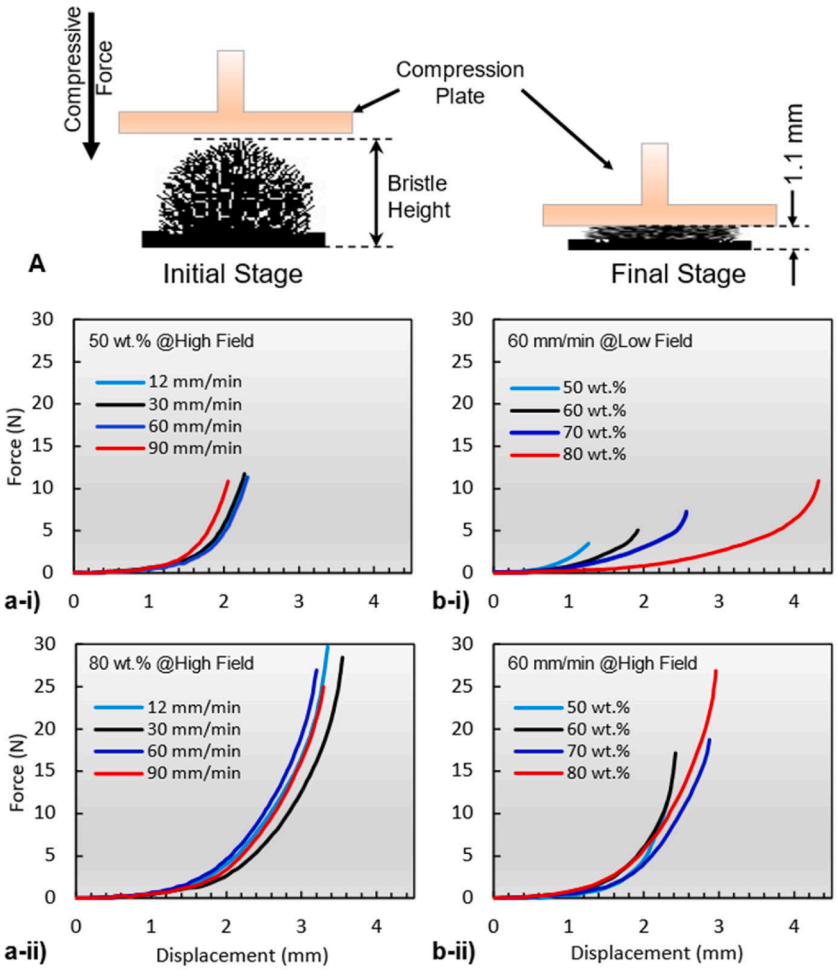

Fig. 3. Force-displacement response of MRF brushes in the presence of a) different strain rates for two selected concentrations of CIP and b) the effect of magnetic flux densities across all concentrations of CIP.

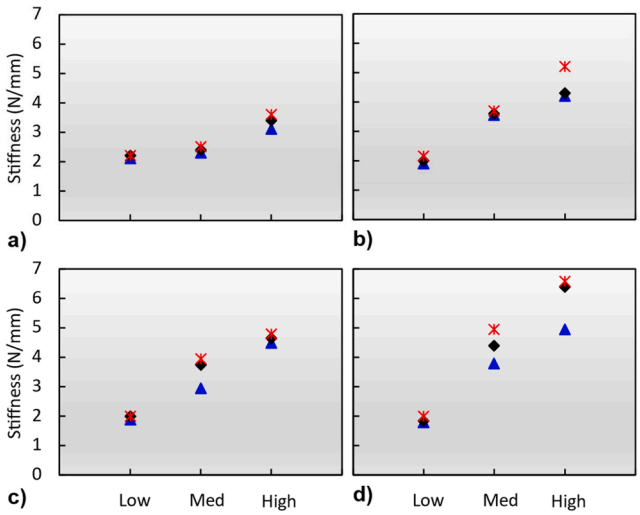

Fig. 4. Plots of stiffness versus magnetic flux density for MRF brush with different CIP concentrations (a) 50 wt.% (b) 60 wt.% (c) 70 wt.% (d) 80 wt.% when subjected to a 60 mm/min compression rate. The symbols (black, red, and blue dots) represent different samples and indicate the variability among them.

the stiffness of the brushes, which can be marked by the dependency of the slope with respect to the concentration of CIP.

In the literature, the mechanical and rheological properties of MR materials are reported to vary non-linearly with the magnetic field strength [54,55]. One study reported the yield stress of MRF increased with $B^{3/2}$, where B is the magnetic flux density [55]. Such non-linear behaviour in MR materials may be well expressed as power-law relationships, and graphically interpreted using a Log-Log scale. Thus, we propose the use of the Log-Log scale for further analysis of the MR brushes with the proposed definition,

$$\mathrm{Log}_e K = n\mathrm{Log}_e B + C \tag{1}$$

where $\log_e K$ is the effective stiffness and $\log_e B$ is the effective magnetic flux density. Importantly, the constant n, we term as the "Magneto-rheological response index". The MR response index provides an effective means to compare the sensitivity of material properties in the presence of a magnetic field. A higher value of the MR response index n indicates a greater effect of the magnetic field. This method of obtaining the MR response index using a Log-Log scheme is highly suitable to compare the relative behaviour between MRF and MRE brushes, especially because the MR fluid brushes do not exhibit a quantifiable stiffness in the absence of a magnetic field. The MR Index is obtained by plotting the stiffness and magnetic flux density using a log scale and is calculated from the gradient of the linear trend fit. Graphically, the slopes are interpreted as the factor by which the stiffness varies with the change in the magnetic flux density.

Fig. 5 shows the Log-Log plot of stiffness and the magnetic flux density alongside the linear trend line. It was observed that the MR Index increased with higher concentrations of CIP. A tabulation of the MR response indices is provided in Table 2. The MRF brush with the lowest CIP concentration (50 wt.%) showed the lowest MR response index. Similar behaviours of the 60 wt.% and 70 wt.% were observed for their stiffness values and the MR response index. The 80 wt.% MRF samples have the highest stiffness values and MR response index at all the flux densities tested. These findings suggest that the higher concentration of CIP offers greater enhancement of the MR response index rather than increasing the strength of the applied magnetic field. In practical applications, high magnetic flux densities are costly to maintain, especially using electromagnets, and pose greater risks of interference within an enclosed system.

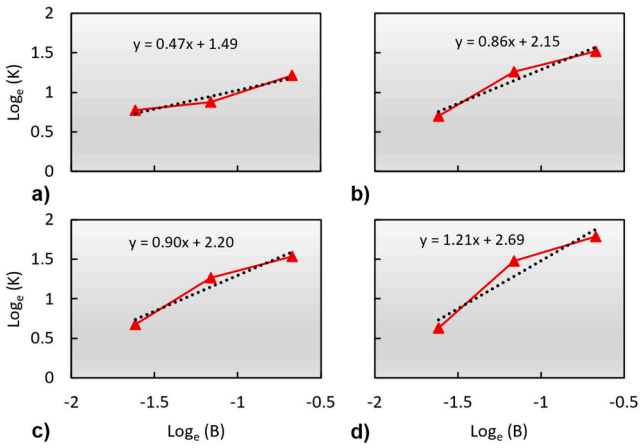

Fig. 5. Plots of effective stiffness versus magnetic flux density using a Log-Log scale for (a) 50 wt.% (b) 60 wt.% (c) 70 wt.% and (d) 80 wt.% MRF brushes.

Table 2
Summary of the MR response indices of MRF brushes with varying concentrations of CIP.

Concentration of CIP	MR response index (n)
50 wt.%	0.47
60 wt.%	0.86
70 wt.%	0.90
80 wt.%	1.21

3.2. Magnetorheological elastomer brushes

Four concentrations of MRE brushes were prepared to compare the results with MRF. However, the higher concentrations of MRE brushes with 70 wt.% and 80 wt.% were found to be unsuitable due to the brittleness of the columnar chains. This resulted in fracture of these specimens, as shown in Fig. 6. Consequently, a high CIP concentration of MRE brushes would not be suitable although higher loading of magnetic fillers for MRE brushes may be achieved by exchanging to a more compliant elastomeric matrix with greater elongation to failure. Conversely, with lower concentrations of 50 wt.% and 60 wt.% CIP, this pattern was not observed, and the brush structure remained intact throughout the test. Furthermore, the results and discussion will only consider the 50 wt.% and 60 wt.% MRE brushes.

The effect of the flux density during the curing of the MRE brushes was examined using an optical microscope and is shown in Fig. 7. The bristle structures are visibly different within the three curing magnetic flux densities. Samples cured under a higher flux density possess fine

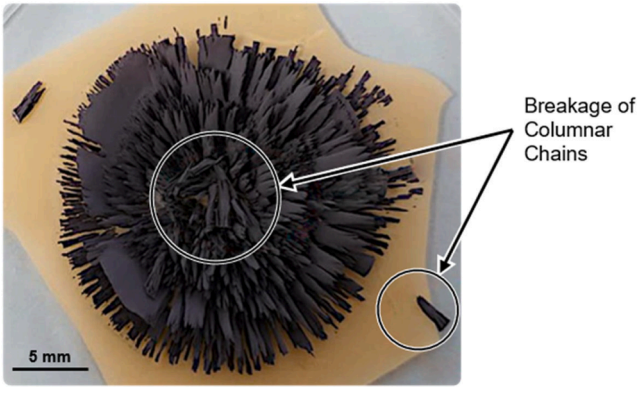

Fig. 6. Fracture and separation of the bristles for 80 wt.% CIP MRE brush cured under Med Field.

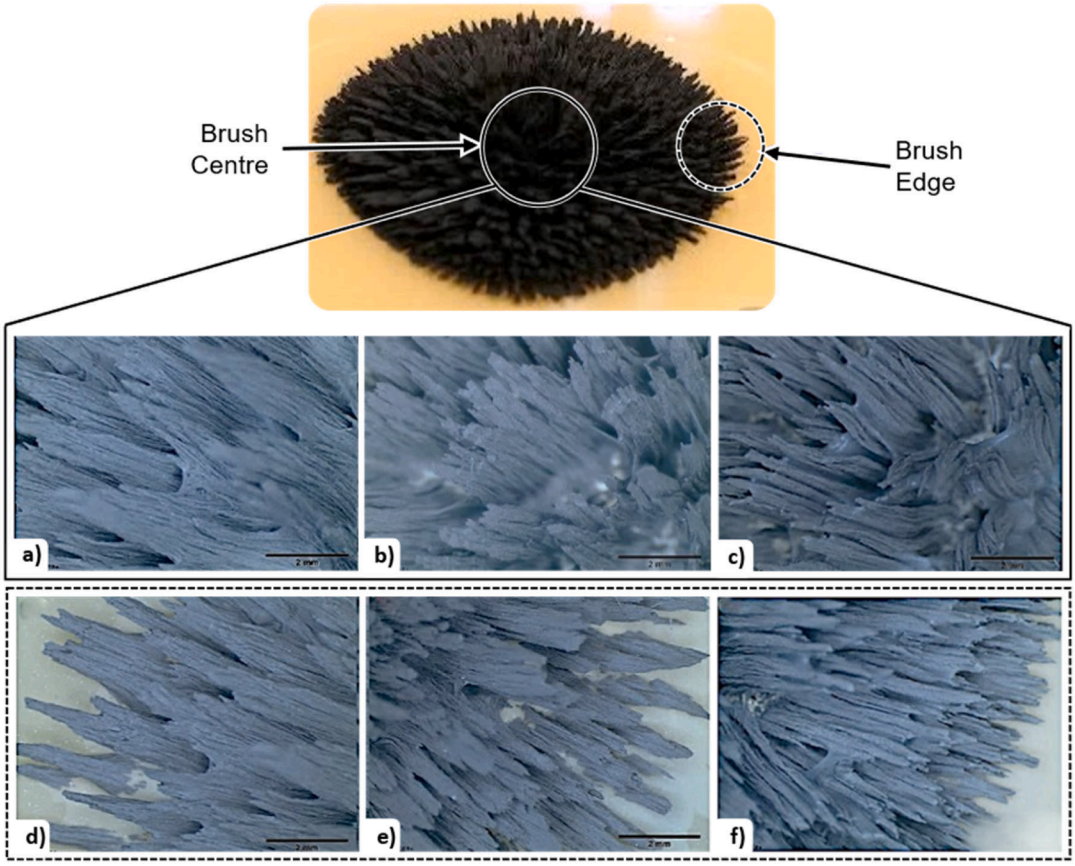

Fig. 7. Optical microscopy of MRE brushes with 50 wt.% CIP located at the centre of the MRE brush cured at (a) Low (b) Med (c) High, and at the edge of the MRE brush cured at (d) Low, (e) Med (f) and High Fields.

columnar bristles (Fig. 7c). The individual bristles are more pronounced with regular column shapes and uniform distribution. The microscopy images captured at the sample edges (Fig. 7f) show similar formation of fine bristles.

The magnetic flux density influences the formation of the bristles due to the competition between gravitational, viscous and magnetic forces along with surface tension. At high flux densities, it is anticipated that the magnetic force dominates across all the interacting forces, thus making the magnetic particles preferentially align, giving rise to uniform and regular-shaped bristles. However, such an interesting phenomenon has to be understood via in-situ investigation and numerical modelling which is not within the scope of this work.

The effect of CIP concentration on the formation of the MRE brushes is shown in Fig. 8. The lower CIP concentration (50 wt.%) brushes consist of finer and more clustered bristles compared to the higher CIP concentration brush. These results align with observations in the literature for anisotropic MREs that use different concentrations of CIP when cured with varying flux densities [56].

Similar to the MRF brush, the compression rate did not significantly influence the force-displacement response of the MRE brushes and their corresponding stiffness. Therefore, the results and analysis reported are based on a 60 mm/min compression rate for 50 wt.% and 60 wt.% MRE brushes. Unlike, the MRF brush, the bristles remain stiff in the absence of a magnetic field and accordingly the results incorporate this state.

Similar to the MRF brushes, the stiffness values were obtained from the force-displacement curves. The absolute stiffness is plotted against the applied flux density and is shown in Fig. 9. MRE brushes with a higher concentration of CIP possess a higher absolute stiffness in the

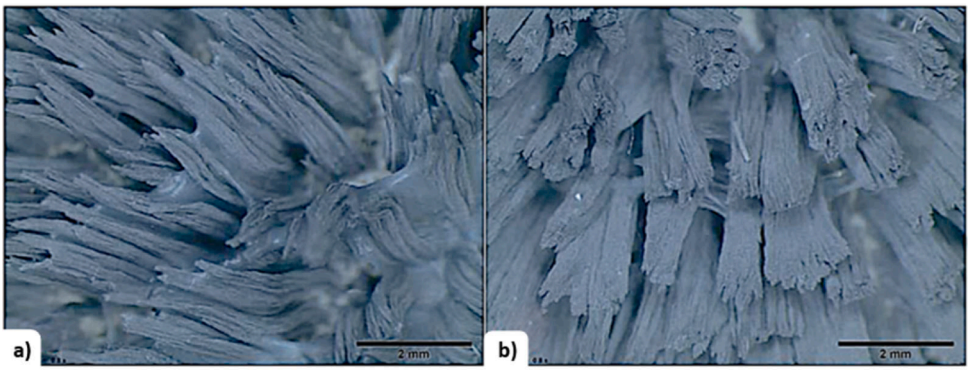

Fig. 8. Optical microscopy taken at the centre of the sample of MRE brushes when cured at High Field for (a) 50 wt.% and (b) 60 wt.% CIP.

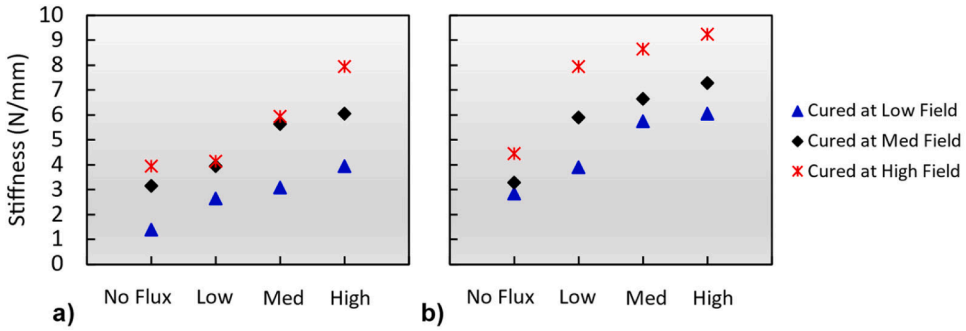

Fig. 9. The effective stiffness plotted against magnetic flux density of MRE brushes: (a) 50 wt.% and (b) 60 wt.% CIP.

presence of a magnetic field. Furthermore, the MRE brush cured at the High Field demonstrates the highest absolute stiffness in the presence of a magnetic field. This behaviour is associated with preferential anisotropy entrained within the brush structure induced by the higher magnetic flux density in the curing process. In the absence of a magnetic field, the 60 wt.% is marginally stiffer than 50 wt.% brushes. In this situation, particles tend to form a more ordered configuration leading to an increase in the field-induced stiffness. Such an effect is also observed for anisotropic MRE [56].

Log-Log plots of stiffness versus magnetic flux density alongside the effect of the curing flux density on the MR response are shown in Fig. 10, in conjunction with the calculated MR response indices provided in Table 3. The effect of the magnetic flux density is more prominent in the 50 wt.% MRE brush compared to the 60 wt.% MRE brush. For 50 wt.% brush, the MR Index increases with greater curing flux densities. However, for 60 wt.% MRE brush, the opposite behaviour was observed, where the MR response index decreased with an increased curing flux density. This suggests that when the inherent material stiffness in absence of a magnetic field is lower, a greater increase in MR response index may be observed. This effect is known in the literature and has been widely reported for MRE [10].

MRE brushes possess a unique trait where the MR response index can be programmed into the manufacturing of the material by selective

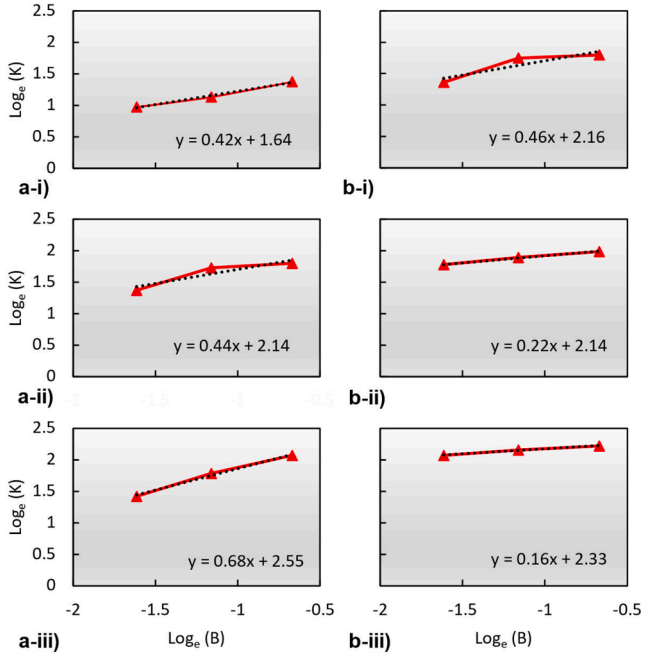

Fig. 10. Plots of the effective stiffness versus magnetic flux density considering the 50 wt.% MRE brush cured at (a-i) Low (a-ii) Med (a-iii) High Field, and for the 60 wt.% MRE brush cured at (b-i) Low (b-ii) Med (b-iii) High Field.

Table 3
Summary of the MR response index of MRE brushes with comparison to MRF brushes.

CIP Concentration	MR response index (n)	
	MRF Brush	MRE Brush
50 wt.%	0.47	0.42 (Low Field Cure) 0.44 (Med Field Cure) 0.68 (High Field Cure)
60 wt.%	0.86	0.46 (Low Field Cure) 0.22 (Med Field Cure) 0.16 (High Field Cure)

control of the curing magnetic flux density. However, for MRF brushes, a higher MR response index was achievable only by using a higher concentration of CIP. The MRE brush with a low concentration of CIP but cured at a higher flux density could demonstrate a similar MR response index as that of the MRF brush with a higher concentration of CIP, as shown in Table 3.

It is plausible to compare the absolute stiffness of the solid and fluid MR brushes because they were created with the same MR volume and tested under the same conditions. When the absolute effective stiffness is compared, the MRF brushes (exposed to a magnetic field) remain just as stiff as their MRE counterparts without the presence of a magnetic field. Furthermore, the MRF brushes also remain weaker than the MRE brushes even when the magnetic field is applied. However, it should be noted that the MR response is greater for MRF brushes.

As given in Table 2, the MRE brush with 50 wt.% CIP demonstrates a higher MR response than that of MRF brush provided that the MRE bristles are formed by curing at High Field. Whereas the MRE brush for 60 wt.% CIP, irrespective of curing magnetic field, remains less responsive than the MRF counterpart. This behaviour is attributed to the initial stiffness of the MRE brush. Specifically, materials with lower stiffness (soft materials), offer the potential to exhibit a broader MR response [57].

This study highlights a need for further exploration of the phenomena arising between the choice of components used in the magnetic elastomeric composite and the formation of bristles owing to the mobility of magnetic particles. Understanding the formation and resultant morphology of the bristle structure and their effect on both static and dynamic stiffness would offer valuable insight. The effect of material composition and magnetic field on the formation of the bristles and their distribution requires further consideration to fully understand the properties and potential applications of MR brushes. In particular, the use of a low modulus matrix material for the MRE brush is expected to amplify the MR response. The ability to program the MR response during the fabrication of the MRE brushes by altering the magnetic field during curing enables optimising the response of the structure with a tuneable stiffness. Coupled with exploring manufacturing processes beyond drop-casting, for example, additive manufacturing has the potential to offer greater control over the formation of bristles, hence, the properties of

MR brushes.

A direct comparison between fluid and elastomeric brushes remains challenging, especially within unconfined volume or non-encapsulated specimens. However, the MR response index provides an informative metric to compare their responsiveness. Importantly, this metric removes the dependency on the bristle geometry of the brush induced by the magnetic field and equally could be applied to other properties of the material.

4. Conclusions

Magnetorheological fluid and solid elastomer brushes were fabricated to investigate the formation of their structures and the magnetorheological response under compressive loading when subjected to an external magnetic field. Magnetorheological fluid and elastomer brushes were produced with concentrations of CIP varying from 50 to 80 wt.%, with the elastomeric equivalents cured under three magnetic flux densities. MRE brushes manufactured with 70 and 80 wt.% CIP were observed to be structurally weak and susceptible to damage, with the bristles breaking during compression testing. Experiments, therefore, focused on 50 and 60 wt.% brush configurations. For comparison of the magnetorheological response between MRE and MRF brushes on their stiffness, a metric termed the MR response index was proposed. From the investigation, a summary of key findings are:

MRE brushes always exhibit a higher absolute stiffness compared to MRF brushes in both absence and the presence of a magnetic field.

- MR response index increases with the concentration of CIP for MRF brushes.
- Both the MR response index and stiffness of the MRE brushes increase with a greater curing flux density.
- MR response index of MRE brush could be higher than MRF brush when cured at high magnetic flux density, however, it was only observed for the 50 wt.% brush.
- The MR response index decreased with an increased curing flux density for 60 wt.% MRE brush associated with the off-state (absence of a magnetic field) stiffness of the MRE brush.

Based on this investigation, MRE brushes with a low concentration of CIP provide an attractive alternative to MRF brushes. The ability to control and tune the curing field strengths when fabricating MRE offer the ability to optimise the MR response and importantly control the formation of the brush structure, including the length, thickness, and density of bristle clusters. Additionally, MRE exhibit a higher initial modulus preferential for structural applications.

A direct comparison of fluid and solid brushes is a challenging task. Therefore, future studies should consider low stiffness compliant material for MRE brushes to contribute further knowledge. Nonetheless, the approach whereby obtaining the MR response index as reported in this study provides a valuable metric to compare the properties across fluid and solid brushes.

The results of this study indicate that the highest concentration of filler materials may not always be required to achieve an optimal response in MR materials. Instead, careful attention to process parameters and the form of the materials themselves could lead to controlled and enhanced functionality. Moreover, the integration of fluid and elastomeric materials could create functionally graded material systems targeting soft robotics applications. Such functionally graded structures could be developed using AM processes which offer the ability to manufacture with greater design freedoms. In addition, computational modelling can be instrumental in developing further understanding of the behaviour of MR bristles and aiding in the design and optimization process of magnetic brushes during fabrication.

In future studies, we aim to integrate computational modelling in conjunction with Additive Manufacturing to produce multifunctional magnetic field responsive materials.

CRediT authorship contribution statement

A.K. Bastola: Conceptualization, Investigation, Methodology, Formal analysis, Writing – original draft, Writing – review & editing. **M Gannavarapu:** Investigation, Formal analysis, Writing – original draft. **L.A. Parry:** Formal analysis, Writing – original draft, Writing – review & editing. **M. Shrestha:** Writing – original draft, Writing – review & editing.

Declaration of Competing Interest

The authors declare that they have no known competing financial interests or personal relationships that could have appeared to influence the work reported in this paper.

Data availability

Data will be made available on request.

References

[1] Y. Kim, X. Zhao, Magnetic Soft Materials and Robots, Chem. Rev. 122 (2022) 5317–5364.
[2] R. Ahamed, S.-B. Choi, M.M. Ferdaus, A state of art on magneto-rheological materials and their potential applications, J. Intell. Mater. Syst. Struct. 29 (2018) 2051–2095.
[3] D. Lc, Model of magnetorheological elastomers, J. Appl. Phys. 85 (1999) 3348–3351.
[4] J. Rabinow, The magnetic fluid clutch, Electr. Eng. 67 (1948) 1167.
[5] J.M., Ginder M.E. Nichols, L.D. Elie, J.L. Tardiff, Magnetorheological elastomers: properties and applications. Smart Struct. Mater. 1999 Smart Mater. Technol., vol. 3675, SPIE, 1999, p. 131–8.
[6] P. Chen, H. Wu, W. Zhu, L. Yang, Z. Li, C. Yan, et al., Investigation into the processability, recyclability and crystalline structure of selective laser sintered Polyamide 6 in comparison with Polyamide 12, Polym. Test. 69 (2018) 366–374, https://doi.org/10.1016/j.polymertesting.2018.05.045.
[7] C. Kadapa, M. Hossain, A unified numerical approach for soft to hard magneto-viscoelastically coupled polymers, Mech. Mater. 166 (2022) 104207, https://doi.org/10.1016/j.mechmat.2021.104207.
[8] E. Yarali, M. Ali Farajzadeh, R. Noroozi, A. Dabbagh, M.J. Khoshgoftar, M. J. Mirzaali, Magnetorheological elastomer composites: Modeling and dynamic finite element analysis, Compos. Struct. 254 (2020) 112881, https://doi.org/10.1016/j.compstruct.2020.112881.
[9] H. Böse, T. Gerlach, J. Ehrlich, Magnetorheological elastomers—An underestimated class of soft actuator materials, J. Intell. Mater. Syst. Struct. 32 (2021) 1550–1564.
[10] A.K. Bastola, M. Hossain, A review on magneto-mechanical characterizations of magnetorheological elastomers, Compos. Part B Eng. 200 (2020) 108348, https://doi.org/10.1016/j.compositesb.2020.108348.
[11] A.K. Bastola, M. Hossain, The shape – morphing performance of magnetoactive soft materials, Mater. Des. 211 (2021) 110172, https://doi.org/10.1016/j.matdes.2021.110172.
[12] Y. Li, J. Li, W. Li, H. Du, A state-of-the-art review on magnetorheological elastomer devices, Smart Mater. Struct. 23 (2014), 123001.
[13] LORD Corporation. Magneto-Rheological (MR) Fluid, 2010.
[14] J.R. Morillas, J. de Vicente, Magnetorheology: a review, Soft Matter 16 (2020) 9614–9642.
[15] M.R. Jolly, J.D. Carlson, B.C. Munoz, A model of the behaviour of magnetorheological materials, Smart Mater. Struct. 5 (1996) 607.
[16] K. Chen, K. Nagashima, S. Takahashi, T. Komatsuzaki, M. Kawai, T. Mitsumata, Magnetically Tunable Transmissibility for Magneto-Responsive Elastomers Consisting of Magnetic and Nonmagnetic Particles, ACS Appl. Polym. Mater. 4 (2022) 2917–2924, https://doi.org/10.1021/acsapm.2c00181.
[17] C. Shen, M. Matsubara, T. Masui, H. Kishimoto, S. Yamanaka, A. Muramatsu, et al., Magnetorheological Elastomer Films with Controlled Anisotropic Alignment of Polystyrene-Modified Fe3O4 Nanoplates, ACS Appl. Polym. Mater. 4 (2022) 7240–7249, https://doi.org/10.1021/acsapm.2c01096.
[18] G.Z. Lum, Z. Ye, X. Dong, H. Marvi, O. Erin, W. Hu, et al., Shape-programmable magnetic soft matter, Proc. Natl. Acad. Sci. 113 (2016) E6007–E6015.
[19] E.Y. Kramarenko, A.V. Chertovich, G.V. Stepanov, A.S. Semisalova, L.A. Makarova, N.S. Perov, et al., Magnetic and viscoelastic response of elastomers with hard magnetic filler, Smart Mater. Struct. 24 (2015) 35002, https://doi.org/10.1088/0964-1726/24/3/035002.
[20] V.G. Shevchenko, G.V. Stepanov, E.Y. Kramarenko, Dielectric Spectroscopy of Hybrid Magnetoactive Elastomers, Polym (2021) 13, https://doi.org/10.3390/polym13122002.
[21] Y. Kim, H. Yuk, R. Zhao, S.A. Chester, X. Zhao, Printing ferromagnetic domains for untethered fast-transforming soft materials, Nature 558 (2018) 274–279.
[22] R. Domingo-Roca, J.C. Jackson, J.F.C. Windmill, 3D-printing polymer-based permanent magnets, Mater. Des. 153 (2018) 120–128.

[23] B. da Costa, L. Linn, K. Danas, L. Bodelot, Towards 4D Printing of Very Soft Heterogeneous Magnetoactive Layers for Morphing Surface Applications via Liquid Additive Manufacturing, Polym (2022) 14, https://doi.org/10.3390/polym14091684.
[24] A.K. Bastola, M. Paudel, L. Li, Development of hybrid magnetorheological elastomers by 3D printing, Polym (United Kingdom) (2018) 149, https://doi.org/10.1016/j.polymer.2018.06.076.
[25] V.Q. Nguyen, A.S. Ahmed, R.V. Ramanujan, Morphing Soft Magnetic Composites, Adv. Mater. 24 (2012) 4041–4054, https://doi.org/10.1002/adma.201104994.
[26] Y. Kim, G.A. Parada, S. Liu, X. Zhao, Ferromagnetic soft continuum robots, Sci. Rob. 4 (2019) eaax7329.
[27] Q. Jiang, P. Zhang, Z. Yu, H. Shi, D. Wu, H. Yan, et al., A review on additive manufacturing of pure copper, Coatings (2021) 11, https://doi.org/10.3390/coatings11060740.
[28] P. Pei, Y. Peng, Constitutive modeling of magnetorheological fluids: A review, J. Magn. Magn. Mater. (2022) 169076.
[29] G. Liu, G.A.O. Fei, D. Wang, W.-H. Liao, Medical applications of magnetorheological fluid: a review, Smart Mater. Struct. (2022).
[30] S.-B. Choi, W. Li, M. Yu, H. Du, J. Fu, P.X. Do, State of the art of control schemes for smart systems featuring magneto-rheological materials, Smart Mater. Struct. 25 (2016) 43001.
[31] K. Danas, S.V. Kankanala, N. Triantafyllidis, Experiments and modeling of iron-particle-filled magnetorheological elastomers, J. Mech. Phys. Solids 60 (2012) 120–138, https://doi.org/10.1016/j.jmps.2011.09.006.
[32] O. Stolbov, Y. Raikher, Large-Scale Shape Transformations of a Sphere Made of a Magnetoactive Elastomer, Polym (2020) 12, https://doi.org/10.3390/polym12122933.
[33] M.A.F. Johari, S.A. Mazlan, N.NA. Ubaidillah, S.A. Abdul Aziz, N. Johari, et al., Shear band formation in magnetorheological elastomer under stress relaxation, Smart Mater. Struct. 30 (2021) 45015, https://doi.org/10.1088/1361-665x/abea03.
[34] M.S. Yusoff, N.A. Yunus, N. Muhammad Zaki, S.A. Mazlan, S.A. Abdul Aziz, Ubaidillah, et al., Comprehensive study on physicochemical characteristics of magnetorheological elastomer featuring epoxidized natural rubber, Smart Mater. Struct. 31 (2022) 55017, https://doi.org/10.1088/1361-665x/ac6347.
[35] M. Kumar, A. Kumar, A. Alok, M. Das, Magnetorheological method applied to optics polishing: A review. IOP Conf. Ser. Mater. Sci. Eng., vol. 804, IOP Publishing, 2020, p. 12012.
[36] S. Kumar, V.K. Jain, A. Sidpara, Nanofinishing of freeform surfaces (knee joint implant) by rotational-magnetorheological abrasive flow finishing (R-MRAFF) process, Precis. Eng. 42 (2015) 165–178.
[37] X. Huang, A. Mohla, W. Hong, A.F. Bastawros, X.-Q. Feng, Magnetorheological brush–a soft structure with highly tuneable stiffness, Soft Matter 10 (2014) 1537–1543.
[38] Y. Zhang, J.F. Zhi, Y.W. Yu, X.X. Zhu, W. Zuo, Study of magnetorheological brush finishing (MRBF) for concave surface of conformal optics. Adv. Mater. Res., vol. 497, Trans Tech Publ, 2012, p. 170–5.
[39] V.K. Jain, P. Ranjan, V.K. Suri, R. Komanduri, Chemo-mechanical magneto-rheological finishing (CMMRF) of silicon for microelectronics applications, CIRP Ann. 59 (2010) 323–328.
[40] J. Zhang, A. Chaudhari, H. Wang, Surface quality and material removal in magnetic abrasive finishing of selective laser melted 316L stainless steel, J. Manuf. Process 45 (2019) 710–719, https://doi.org/10.1016/j.jmapro.2019.07.044.
[41] Y. Zou, H. Xie, C. Dong, J. Wu, Study on complex micro surface finishing of alumina ceramic by the magnetic abrasive finishing process using alternating magnetic field, Int. J. Adv. Manuf. Technol. 97 (2018) 2193–2202, https://doi.org/10.1007/s00170-018-2064-0.
[42] A. Babbar, C. Prakash, S. Singh, M.K. Gupta, M. Mia, C.I. Pruncu, Application of hybrid nature-inspired algorithm: Single and bi-objective constrained optimization of magnetic abrasive finishing process parameters, J. Mater. Res. Technol. 9 (2020) 7961–7964, https://doi.org/10.1016/j.jmrt.2020.05.003.
[43] H. Lu, M. Zhang, Y. Yang, Q. Huang, T. Fukuda, Z. Wang, et al., A bioinspired multilegged soft millirobot that functions in both dry and wet conditions, Nat. Commun. 9 (2018) 1–7.
[44] E.B. Joyee, A. Szmelter, D. Eddington, Y. Pan, 3D printed biomimetic soft robot with multimodal locomotion and multifunctionality, Soft Robot 9 (2022) 1–13.
[45] M.J. Oh, A. Babeer, Y. Liu, Z. Ren, J. Wu, D.A. Issadore, et al., Surface Topography-Adaptive Robotic Superstructures for Biofilm Removal and Pathogen Detection on Human Teeth, ACS Nano (2022), https://doi.org/10.1021/acsnano.2c01950.
[46] M.A. Moreno-Mateos, J. Gonzalez-Rico, E. Nunez-Sardinha, C. Gomez-Cruz, M. L. Lopez-Donaire, S. Lucarini, et al., Magneto-mechanical system to reproduce and quantify complex strain patterns in biological materials, Appl. Mater. Today 27 (2022) 101437, https://doi.org/10.1016/j.apmt.2022.101437.
[47] Y. Shou, L. Liu, Q. Liu, Z. Le, K.L. Lee, H. Li, et al., Mechano-responsive hydrogel for direct stem cell manufacturing to therapy, Bioact. Mater. 24 (2023) 387–400, https://doi.org/10.1016/j.bioactmat.2022.12.019.
[48] A. Malas, E. Saleh, M. del C. Giménez-López, G.A. Rance, T. Helps, M. Taghavi, et al., Reactive Jetting of High Viscosity Nanocomposites for Dielectric Elastomer Actuation, Adv. Mater. Technol. 7 (2022) 2101111, https://doi.org/10.1002/admt.202101111.
[49] Q. Hu, G.A. Rance, G.F. Trindade, D. Pervan, L. Jiang, A. Foerster, et al., The influence of printing parameters on multi-material two-photon polymerisation based micro additive manufacturing, Addit. Manuf. 51 (2022) 102575, https://doi.org/10.1016/j.addma.2021.102575.
[50] J.-H. Groth, C. Anderson, M. Magnini, C. Tuck, A. Clare, Five simple tools for stochastic lattice creation, Addit. Manuf 49 (2022) 102488, https://doi.org/10.1016/j.addma.2021.102488.
[51] M. Rafiee, R.D. Farahani, D. Therriault, Multi-material 3D and 4D printing: a survey, Adv. Sci. 7 (2020) 1902307.
[52] M.L. Lopez-Donaire, G. de Aranda-Izuzquiza, S. Garzon-Hernandez, J. Crespo-Miguel, M. Fernandez-de la Torre, D. Velasco, et al., Computationally Guided DIW Technology to Enable Robust Printing of Inks with Evolving Rheological Properties, Adv. Mater. Technol. 8 (2023) 2201707, https://doi.org/10.1002/admt.202201707.
[53] G. Schubert, P. Harrison, Large-strain behaviour of Magneto-Rheological Elastomers tested under uniaxial compression and tension, and pure shear deformations, Polym. Test 42 (2015) 122–134, https://doi.org/10.1016/j.polymertesting.2015.01.008.
[54] E. Esmaeilnezhad, H. Jin Choi, M. Schaffie, M. Gholizadeh, M. Ranjbar, Kwon S. Hyuk, Rheological analysis of magnetite added carbonyl iron based magnetorheological fluid, J. Magn. Magn. Mater. 444 (2017) 161–167, https://doi.org/10.1016/j.jmmm.2017.08.023.
[55] S. Genç, P.P. Phulé, Rheological properties of magnetorheological fluids, Smart Mater. Struct. 11 (2002) 140–146, https://doi.org/10.1088/0964-1726/11/1/316.
[56] L. Chen, X.L. Gong, W.H. Li, Microstructures and viscoelastic properties of anisotropic magnetorheological elastomers, Smart Mater. Struct. 16 (2007) 2645–2650, https://doi.org/10.1088/0964-1726/16/6/069.
[57] A. Stoll, M. Mayer, G.J. Monkman, M. Shamonin, Evaluation of highly compliant magneto-active elastomers with colossal magnetorheological response, J. Appl. Polym. Sci. 131 (2014), https://doi.org/10.1002/app.39793.